Springer

KSME

Journal of Mechanical Science and Technology 33 (7) (2019) 3509~3519
www.springerlink.com/content/1738-494x(Print)/1976-3824(Online)
DOI 10.1007/s12206-019-0645-y

# Design of general-purpose assistive exoskeleton robot controller for upper limbs †

Hwiwon Seo[1] and Sangyoon Lee[2,*]

[1]Department of Mechanical Design and Production Engineering, Konkuk University, Seoul, Korea
[2]School of Mechanical Engineering, Konkuk University, Seoul, Korea

(Manuscript Received February 13, 2019; Revised March 28, 2019; Accepted April 11, 2019)

**Abstract**

Though research and development on exoskeleton robots have been active recently, the results have limitations in terms of independence from robot platforms and capability for general purposes. This paper presents a novel control scheme named the general-purpose assistive exoskeleton controller (GAEC) for upper limb assistive exoskeleton robots. With only the joint position information used, GAEC is designed to be applicable to any type of upper limb exoskeleton robot platform assisting human worker's common activities. GAEC works in two modes: (1) An external force is neutralized by generation of force with the same magnitude and the opposite direction. (2) The control system complies with the user's own force while maintaining the force that compensates for the external force neutralized in the first mode. In addition to theoretical description of the controller, computer simulation was conducted for validation using a robot model adopted from related studies. Two exemplary working scenarios were considered in the simulation: lifting and moving an object, and tightening a bolt with a wrench.

*Keywords*: Exoskeleton robot controller; General-purpose assistive exoskeleton; Terminal sliding mode control; Upper limb exoskeleton robot

## 1. Introduction

Various research studies for developing and applying assistive exoskeleton robots have been reported [1-33]. Exoskeleton robots are designed to improve the user's physical performance in many fields where human's physical labor is required, such as manufacturing, construction, rescue, and military operations. In particular, upper limb exoskeletons for supporting the user's upper body in various tasks are very useful.

Development of an upper limb exoskeleton involves two main issues. One is design of the mechanical structure. Biomechanics of humans, such as parameters of limb links, joint center of rotation, and body segment dimension, contains a large variance and is also difficult to capture [24]. Incompatibility between biomechanics of human arm and mechanical structure of exoskeletons causes misalignments, which leads to the user's discomfort and limits the user's natural movement [24].

The second issue is design of the controller. An assistive exoskeleton robot is supposed to follow the user's intended motion, while rejecting external disturbances. However, capturing the user's motion intention exactly is still at research level [25]. This paper is focused on the controller design issue.

*Corresponding author. Tel.: +82 2 450 3731
E-mail address: slee@konkuk.ac.kr
† Recommended by Editor Ja Choon Koo


Control schemes for upper limb exoskeletons can be categorized into two types: Biological signal-based and non-biological signal-based [25]. Electro-myography (EMG) is often used in the first type. This type of control scheme estimates the user's motion intention by classifying the EMG signal using neuro-fuzzy, fuzzy logic, and neural network techniques, or muscle model-based methods [26]. However, the use of EMG signals involves difficulties in terms of sensor placement, signal processing, and controller implementation [27]. Instead of using EMG, some researchers attempted to capture the user's motion intention by observing changes in muscle density [2] or muscle volume [4].

Non-biological signal-based control schemes use force or torque signals. This type of control scheme estimates the user's motion intention by analyzing the user's force on the robot. To obtain the user's force information, force/torque sensors can be set on a handle that the user grasps for manipulating the robot [9, 11, 12]. Force/torque sensors can be used in a different form in Ref. [10] where the sensors were designed as a ring-shaped arm coupling covering the arm. The use of force/torque sensors causes difficulties in locating the sensor and disadvantage in cost and size [25]. Thus, control schemes that use an observer instead of force/torque sensors have been proposed [13].

With regard to applications of existing upper limb exoskeleton robots, another limitation can be found. Some research studies were focused on optimizing performance of the robot in a specific application field or task, rather than covering human worker's common activities [7, 8, 14]. Additional problem is found in exoskeleton devices that use passive elements only. Most of them compensate for the weight of the user's particular body parts and were developed for use in industry [28]. These exoskeletons are light weight and low price, but their usage is limited and their performance is optimized only for a specific weight [29]. Recently, studies about soft wearable assistive robots that replace rigid structures with soft materials were reported [30-33]. These robots have advantage in wearability and misalignment problem, however, assistive force is limited due to lack of rigid structures.

In this paper, a novel control scheme for an upper limb assistive exoskeleton robot, named the general-purpose assistive exoskeleton controller (GAEC), is proposed. The controller is designed to assist human worker's common activities and also designed to be independent of the type of exoskeleton robot platform. The term "human worker's common activities" refers to activities that humans often do repeatedly in a working environment, such as carrying, pushing/pulling an object, and maintaining a certain body posture. Many activities found in industry [34-36] can be categorized into those activities.

Rather than trying to estimate the user's motion intention, GAEC complies only with the user's own force while compensating for the other forces. Thus, sensor systems for observing and analyzing the user's motion intention are not needed. GAEC requires only the joint position information, which makes it applicable to any exoskeleton robot platform where measurable joint positions are available.

This paper is organized as follows. In Sec. 2, a human-robot system model and dynamic equation used in the design of GAEC are introduced. Sec. 3 presents the concept and design of GAEC. GAEC was implemented and simulated using a robot model adopted from a related study. In Sec. 4, the simulation results are provided and discussed. Finally, the conclusion is presented in Sec. 5.

## 2. System modeling

Fig. 1 depicts the typical *n*-degrees of freedom (DOFs) exoskeleton robot system. The robot is assumed to be fixed at the base, which can be a backpack or a spine module, etc. Kinematics of the user is not considered because of its uncertainty and variability. Instead, only the user's force through the coupling is considered. Point $\hat{p}$ on the user's hand in Fig. 1 indicates where the external force $F_e$ is expected to be applied. If the robot is equipped with a specific tool, the tool position corresponds to $\hat{p}$. Point $p$ in Fig. 1 indicates where the actual external force is applied. It may not coincide with $\hat{p}$ and may not be a fixed point.

Note that the user's force $\tau_h$ is expressed as a joint space force like the robot's force $\tau_r$. In fact, the user's force is a work space force transmitted through the coupling. However, because the user knows intuitively how to manipulate the robot through the user's body, the user's force that is converted into

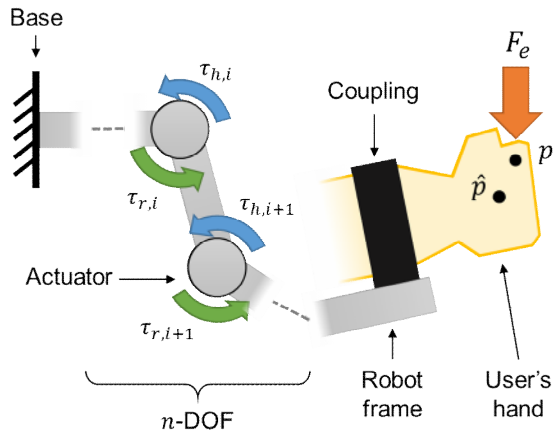


Fig. 1. Typical exoskeleton robot system model.

joint space will eventually lead to the desired motion. Therefore, it is convenient to consider the user's force as a joint space force. The external force is an unknown and unpredictable force from an external environment, and therefore, is expressed as a work space force.

Dynamics of the exoskeleton system can be written as

$$D(q)\ddot{q} + C(q,\dot{q})\dot{q} + g(q) = \tau_r + \tau_h + J^T(q)F_e \quad (1)$$

where $q \in \mathbb{R}^{n\times 1}$ is the joint position, $D(q) \in \mathbb{R}^{n\times n}$ is the inertia matrix, $C(q,\dot{q}) \in \mathbb{R}^{n\times n}$ is the Corilolis force and centrifugal term, $g(q) \in \mathbb{R}^{n\times 1}$ is the gravity term. In Eq. (1), $\tau_r$, $\tau_h \in \mathbb{R}^{n\times 1}$ represents the generalized force exerted by the robot and user, respectively, $J(q) \in \mathbb{R}^{6\times 1}$ is the Jacobian matrix of the point $p \in \mathbb{R}^{3\times 1}$, and $F_e \in \mathbb{R}^{6\times 1}$ is the external work space force.

Total inertia of the system consists of inertia of the robot, user, and external source, if an object is being held. Thus, $D(q)$, $C(q,\dot{q})$, and $g(q)$ are

$$\begin{aligned} D(q) &= D_r(q) + D_h(q) + D_e(q) \\ C(q,\dot{q}) &= C_r(q,\dot{q}) + C_h(q,\dot{q}) + C_e(q,\dot{q}) \\ g(q) &= g_r(q) + g_h(q) \end{aligned} \quad (2)$$

where the subscripts *r*, *h* and *e* denote the robot, user, and external source, respectively. The gravity term does not include the gravity of the external source. This is because it is convenient to include it in the external force term. Note that the user terms may not be obtained exactly. Therefore, the system equation may contain uncertainty.

## 3. Controller design

GAEC is a high-level controller that generates a target force signal, which is realized by each actuator force controller. In the following subsections, the control method, the controller architecture, and the performance of GAEC are discussed.

### 3.1 Method

Exoskeleton robots are supposed to comply with the user's force, while resisting external forces, which can be implemented by position control. Application of position control enables the robot to resist external forces in order to maintain its certain position. Therefore, the robot can be made comply with the user's force by deactivating the position control. However, the problem of distinguishing the source of force using position information only has to be solved.

One approach for resolving this problem is to separate forces by time such that GAEC can work in two modes: (1) The force is assumed to be from an external source, and it is neutralized by the position control. (2) While compensating for the external force, the control system complies with the user's force. In fact, many physical activities are performed similarly to the two-mode process.

If we consider an example of lifting an object, a person first needs to produce force to overcome the weight of the object. Then, the person can move the object by producing an additional force while maintaining the force against the weight. Similarly, for pushing/pulling an object, a person first needs to apply force that can overcome resistive forces such as friction, and then can push/pull the object by producing an additional force.

A couple of things are noted with this approach. First, a discontinuity in the user's behavior is unavoidable. Because the external force is neutralized by the position control, the user cannot move until the neutralization process is over. Secondly, the external force should be given like a step so that the end of the neutralization process can be determined clearly. If magnitude or direction of the external force keeps changing like vibration, the neutralization process cannot be completed.

### 3.2 Architecture

Fig. 2 shows a block diagram of GAEC. The main components are the position controller, double integration loop, external force estimator, and signal switch.

#### 3.2.1 Position controller

The purpose of the position controller is to neutralize external force with position information only. Because the output signal of GAEC is the target force, the output of the position controller is the target force signal to maintain a certain position. It converges to neutralization force with the same magnitude and the opposite direction compared to the external force.

The performance of the position controller in terms of robustness to disturbance and position tracking is critical to performance of GAEC. If the controller works better, the neutralization process takes less time, which results in less discontinuity in behavior. Any type of position controller of the second order or less, linear or nonlinear, can be used. However, to guarantee the performance of the position controller against uncertainty in model parameters and various external forces, an adaptive or robust controller is recommended.

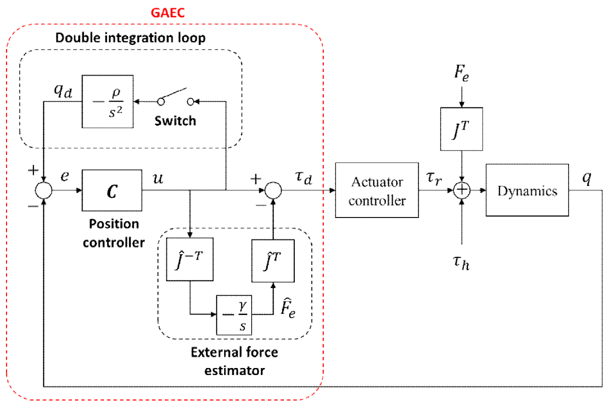


Fig. 2. Block diagram of the control system.

#### 3.2.2 External force estimator

The external force estimator is a kind of proportional integral compensator. For the constant external force $F_e$, the output of the position controller $u \in \mathbb{R}^{n\times 1}$ is accumulated in the integrator until it reaches $F_e$. As shown in Fig. 2, the target force signal $\tau_d \in \mathbb{R}^{n\times 1}$ is written as

$$\tau_d = u - \hat{J}^T(q)\hat{F}_e = u + \gamma \hat{J}^T(q)\hat{J}^{-T}(q)U = u + \gamma U \quad (3)$$

where superscript $T$ denotes the transpose, $\hat{J}(q) \in \mathbb{R}^{n\times 6}$ is the Jacobian matrix of $\hat{p}$, $\gamma$ is a positive constant, and $dU/dt = u$. To simplify the discussion, let us suppose that the actuator controller is designed properly and the user handles the weight of the user and the robot, so that $\tau_r \approx \tau_d$ and $\tau_h = g(q)$. Then, Eq. (1) becomes

$$D(q)\ddot{q} + C(q,\dot{q})\dot{q} = \dot{U} + \gamma U + J^T(q)F_e \quad (4)$$

$$\dot{U} + \gamma U = \{D(q)\ddot{q} + C(q,\dot{q})\dot{q}\} - J^T(q)F_e . \quad (5)$$

Suppose the system is stable, so that $\dot{q} \rightarrow 0$ as $t \rightarrow \infty$. If $\hat{p}$ is chosen such that $\hat{p} \approx p$, Eq. (5) becomes

$$\gamma U = -\hat{J}^T(q)\hat{F}_e \approx -J^T(q)\hat{F}_e = -J^T(q)F_e . \quad (6)$$

Thus, $\hat{F}_e \approx F$ and the external force is neutralized as $t \rightarrow \infty$. As the system is more stable and $\gamma$ is larger, this process takes less time.

Stability of the system can be guaranteed better by adding a dissipation term to the position controller. For a positive constant $K$ and the output of the original position controller $u_0$, let $u = u_0 - K\dot{q}$. Then, $\tau_d$ becomes

$$\tau_d = u_0 + \gamma U_0 - K\dot{q} - \gamma K e \quad (7)$$

where $e = q - q_0$ for the desired steady-state position $q_0$. Let us introduce Lyapunov function candidate as the mechanical energy of the system.

$$V = \tfrac{1}{2}\{\dot{q}^T D(q)\dot{q} + e^T \gamma K e\} . \quad (8)$$

According to the principle of the conservation of mechanical energy, the time derivative of $V$ is equal to the power provided by the applied forces. If $\tau_r \approx \tau_d$,

$$\begin{aligned}\dot{V} &= \dot{q}^T\left\{\tau_r - g(q) + J^T(q)F_e\right\} + \dot{q}^T\gamma K\dot{e} \\ &= \dot{q}^T\left\{u_0 + \gamma U_0 - g(q) + J^T(q)F_e\right\} - \dot{q}^T K\dot{q}\ .\end{aligned} \tag{9}$$

Therefore, by choosing $K$ such that an inequality

$$\left\|\dot{q}^T\left\{u_0 + \gamma U_0 - g(q) + J^T(q)F_e\right\}\right\| \le K\left\|\dot{q}\right\|^2 .$$

to be satisfied, stability of the system is guaranteed.

#### 3.2.3 Double integration

The double integration loop makes the robot comply with the user's force by deactivating the position controller, while maintaining $\hat{F}_e$. This part is inspired by the theory of impulse and momentum. A change in momentum is equal to the impulse:

$$\Delta(mv) = m\Delta v = \int F dt\ . \tag{10}$$

Accordingly, the desired velocity is set at $\dot{q}_d = \int \tau_h dt$. However, because there is no way for measuring the user's force $\tau_h$, it cannot be used directly. Instead, using the property that the output of the position controller reacts to the user's force, $\rho u$ is used, where $\rho$ is a positive constant. Therefore, the desired velocity is set as

$$\dot{q}_d = -\rho\int u dt. \tag{11}$$

Note that the sign is negative since $u$ is a reaction to $\tau_h$. To guarantee stability of $q_d$, a dissipation term can be added, such as

$$\ddot{q}_d = -\rho u - b\dot{q}_d \tag{12}$$

where $b$ is a positive constant.

Consider the following general expression of $u$

$$u \approx \lambda_2\ddot{q}_d + \lambda_1\dot{q}_d + \lambda_0 q_d + \omega(q,\dot{q},\ddot{q}) \tag{13}$$

where $\lambda_0$, $\lambda_1$ and $\lambda_2$ are positive constants or 0. For example, for a simple proportional derivative controller, $\lambda_2 = 0$ and $\omega = -\lambda_1\dot{q} - \lambda_0 q$, so that $u = -\lambda_1\dot{e} - \lambda_0 e$, where $e = q - q_d$. Substituting Eq. (12) into Eq. (13) and differentiating twice, we have

$$\begin{aligned}\ddot{u} &= \lambda_2 q_d^{(4)} + \lambda_1 q_d^{(3)} + \lambda_0\ddot{q}_d + \ddot{\omega} \\ &= -\lambda_2\left(\rho\ddot{u} + bq_d^{(3)}\right) - \lambda_1\left(\rho\dot{u} + b\ddot{q}_d\right) - \lambda_0(\rho u + b\dot{q}_d) + \ddot{\omega} \\ &= -\rho\left(\lambda_2\ddot{u} + \lambda_1\dot{u} + \lambda_0 u\right) - b\left(\lambda_2 q_d^{(3)} + \lambda_1\ddot{q}_d + \lambda_0\dot{q}_d\right) + \ddot{\omega} \\ &= -\rho\left(\lambda_2\ddot{u} + \lambda_1\dot{u} + \lambda_0 u\right) - b(\dot{u} - \dot{\omega}) + \ddot{\omega}\end{aligned}$$

or

$$\rho\left(\lambda_2\ddot{u} + \lambda_1\dot{u} + \lambda_0 u\right) + \left(\ddot{u} + b\dot{u}\right) = \ddot{\omega} + b\dot{\omega} \tag{14}$$

where $q_d^{(n)}$ is $n$-th derivative of $q_d$. For a sufficiently large value of $\rho$, Eq. (14) becomes

$$\lambda_2\ddot{u} + \lambda_1\dot{u} + \lambda_0 u = \tfrac{1}{\rho}\left(\left(\ddot{\omega} + b\dot{\omega}\right) - \left(\ddot{u} + b\dot{u}\right)\right) \approx 0\ . \tag{15}$$

This logic may not work for some nonlinear position controllers. However, effect of the double integration loop can be inferred. Eventually, $u$ approaches 0 as $\lambda_0$, $\lambda_1$, $\lambda_2 \ge 0$, and $\hat{F}_e$ is not updated, because it is the integration of $u$. This makes the robot comply with the user's force while the external force is compensated.

#### 3.2.4 Signal switch

The signal switch determines whether $u$ is to be connected to the double integration loop or not. In other words, when the signal switch is off, the signal through the switch is 0, and when the switch is on, it is $u$. Therefore, according to the discussion in Sec. 3.2.3, when the switch is turned off, $q_d$ is not updated, the position controller starts functioning, and $\hat{F}_e$ is updated. When $q_d$ is fixed in the position controller, the robot cannot be moved. However, when the switch is turned on, because of the double integration loop, the position controller stops functioning and $\hat{F}_e$ is fixed. The robot can be moved in this state while $\hat{F}_e$ is maintained. In summary, the control law of GAEC can be written as

$$\tau_d = \begin{cases} u + \gamma\int u dt & \text{if Switch Off} \\ u_{\text{deact}} - \hat{J}^T(q)\hat{F}_e & \text{if Switch On}\end{cases} \tag{16}$$

where $u_{\text{deact}}$ denotes output of the position controller deactivated by the double integration loop, which is nearly 0.

Thus, when an external force is applied and needs to be neutralized, the switch should be turned off. When the neutralization process is complete and the user wants to move, the signal switch should be switched on. This is done automatically according to the control phases, which is discussed in the next subsection.

### 3.3 Phases

GAEC has three phases. In phase I, external forces are neutralized. When this process is complete, phase II is initiated. Phase II is an intermediate phase between phases I and III and the system waits for the user's force to be applied during phase II. Phase III is initiated when the user's force is applied. The signal switch is turned off in phases I and II but it is turned on in phase III. The robot's motion is allowed in phase III. The end of phase III is the moment when the motion is stopped or changed abruptly, for example, because of envi-

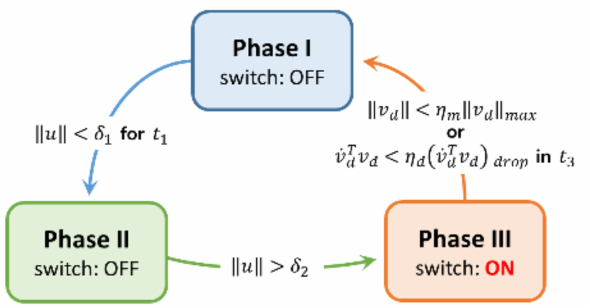

Fig. 3. Cycle of phases.

ronmental constraints or change of the motion intention. In addition, when another external force is applied, it is also considered as the end of phase III. At the end of phase III, the system returns to phase I.

The cycle of phases and its shifting law are depicted in Fig. 3. The shifting law is implemented by evaluating the control signals. The shifting law of phases I and II uses $u$. If $\hat{F}_e$ converges, $u$ also converges to 0. Convergence of $u$ can be determined by observing if the magnitude of $u$ remains smaller than a threshold for a sufficiently long time span. Thus, the shifting law of phase I is defined as

**Shift to phase II if** $\|u\| < \delta_1$ **for** $t_1$

where $\delta_1$ and $t_1$ are positive constants. If $\delta_1$ is too large and $t_1$ is too short, the external force may not be neutralized successfully. If $\delta_1$ is too small and $t_1$ is too large, the robot may not move for a much longer time than necessary. In phase II, considering the applied force is the user's force, the shifting law is defined as

**Shift to phase III if** $\|u\| > \delta_2$

where $\delta_2$ represents a positive constant. If $\delta_2$ is too large, too much force is required to initiate motion, or if $\delta_2$ is too small, the shifting law becomes excessively sensitive.

The shifting law of phase III should be designed such that the end of motion can be determined. This can be achieved by using joint velocity $\dot{q}$. However, to avoid noise, $\dot{q}_d$ can be used instead of $\dot{q}$. Furthermore, it may be more intuitive to use the work space velocity, $v_d = \hat{J}(q)\dot{q}_d$. In general, the velocity reaches the maximum value during a certain motion, and then decreases to 0 as the motion is completed. If $\|v_d\|$ drops below a certain proportion of the maximum value observed, the motion can be considered to have been completed or stopped. A sudden change in the motion can be determined by observing $\dot{v}_d^T v_d = \frac{d}{dt}\left(\frac{1}{2}v_d^{\,2}\right)$, which represents the change in the velocity magnitude. A decrease in this value means force is being applied in the opposite direction to produce motion. If the value drops by a certain proportion in a sufficiently short time, a sudden change in the motion is supposed to occur. Therefore, the shifting law of phase III is defined as

**Shift to phase I if** $\|v_d\| < \eta_m \|v_d\|_{\max}$

**or** $\dot{v}_d^T v_d < \eta_m \left(\dot{v}_d^T v_d\right)_{drop}$ **in** $t_3$

where $\eta_m$ and $\eta_d$ are positive constants between 0 and 1, $t_3$ is a positive constant, $\|v_d\|_{\max}$ is the maximum of observed $\|v_d\|$, and $\left(\dot{v}_d^T v_d\right)_{drop}$ is the value of $\dot{v}_d^T v_d$ when it starts to drop. If $\eta_m$ and $\eta_d$ are too large and $t_3$ is too small, the shifting law becomes too sensitive, or vice versa.

The values of $\delta_1$, $t_1$, $\delta_2$, $\eta_m$, $\eta_d$ and $t_3$ can be determined by observing $\|u\|$, $\|v_d\|$ and $\dot{v}_d^T v_d$. The discontinuity in behavior can be minimized by an appropriate choice of these values. They may have to be tuned or optimized by considering tradeoff. Additional conditions can be applied to the shifting law or a different design of the shifting law is possible.

### 3.4 Residual force

Although the external force is assumed static, each joint experiences a different force as the joint positions change. The external force estimator was designed to resolve this problem by estimating the external force in the workspace, and then converting it into the joint space force. However, this works perfectly only when $\hat{p} = p$. In practice, $\hat{p}$ does not coincide with $p$ most of time. This results in incomplete compensation of the external force, which is called residual force in this paper. During phases I and II, with joint position $q = q_0$, $\hat{F}_e$ converges to

$$\hat{F}_e = \hat{J}_0^{-T} J_0^T F_e \,. \tag{17}$$

according to Eq. (6), where $\hat{J}_0 = \hat{J}(q_0)$ and $J_0 = J(q_0)$. When the system shifts to phase III, with a new joint position $q$, the residual force is

$$F_e - J^{-T}\hat{J}^T\hat{F}_e = (I - J^{-T}\hat{J}^T\hat{J}_0^{-T}J_0^T)F_e = \Delta^T F_e \tag{18}$$

where $I \in \mathbb{R}^{6\times6}$ is the identity matrix, $\hat{J} = \hat{J}(q)$, and $J = J(q)$. The magnitude of the residual force is determined by the matrix $\Delta \in \mathbb{R}^{6\times6}$, and $\Delta$ can be rewritten as

$$\Delta = I - J_0\hat{J}_0^{-1}\hat{J}J^{-1} = \left(J\hat{J}^{-1} - J_0\hat{J}_0^{-1}\right)\left(J\hat{J}^{-1}\right)^{-1}. \tag{19}$$

If $\hat{p} = p$, $J\hat{J}^{-1} = I$ $\forall q$. Thus, $\Delta = 0$ for $\forall q$ only if $\hat{p} = p$.

The gravitational force may also cause the residual force. It is applied to each center of mass of the robot and the user's body parts. Therefore, because the external force estimator considers all forces applied to $\hat{p}$, the residual force cannot be removed perfectly even if $\hat{p} = p$. However, this problem can be solved by employing a gravity compensator.

## 4. Simulation study

Computer simulation was conducted using Matlab for validation of GAEC. Two exemplary working scenarios were examined. In each scenario torque required for the user with the robot's assistance was compared to that without it. The user's torque with the robot's assistance was designed such that desired motion can be accomplished. If there is no desired motion, the user's torque is zero and only the robot's torque works. This can be written as

$$\tau_h = \begin{cases} 0 & \text{if } \dot{q}_h = 0 \\ D(q)\left\{K_1\left(q_h - q\right) + K_2\left(\dot{q}_h - \dot{q}\right)\right\} & \\ +C(q,\dot{q})\dot{q} + g(q) & \text{if } \dot{q}_h \neq 0 \\ +J^T(q)F_e - \tau_r & \end{cases} \tag{20}$$

where $K_1$, $K_2$ are positive constants and $q_h$ is the user's desired position. Note that $q_h$ is different from $q_d$ in the controller. Without the robot's assistance, the user must overcome all the forces alone. The user's torque required to accomplish the same work without the robot's assistance can be written as

$$\tau_h^* = D(q)\left\{K_1\left(q_h - q\right) + K_2\left(\dot{q}_h - \dot{q}\right)\right\} + C(q,\dot{q})\dot{q} + g(q) + J^T(q)F_e\,. \tag{21}$$

Substituting Eq. (20) to Eq. (1), the robot joint position $q$ is computed. And $q_h$ and $F_e$ are defined according to situation in the scenario, and $\tau_r$ is obtained by GAEC. The following subsections present the robot model, implementation of the controller and simulation results. With the robot model, the system dynamics terms $D(q)$, $C(q,\dot{q})$ and $g(q)$ are defined and $\tau_r$ is defined by the implemented controller.

### *4.1 Models*

To show that GAEC is independent of the type of exoskeleton robot platform, this simulation employs a robot model that is adopted from related studies: Ebrahimi's [7, 8, 14] and Schiele's [37] exoskeletons. Ebrahimi's one actively supports 3 DOFs in the arm: Shoulder abduction/adduction, flexion/extension, and elbow flexion/extension. The remaining DOFs are freely movable by passive joints. The arm coupling is placed on both upper and lower arms. The spinal module to which the arm part is attached is mounted on the torso.

Schiele's exoskeleton is a non-anthropomorphic one where its arm part is attached under the chest. It has 8 active joints that generate torque corresponding to every rotation of the shoulder and wrist and flexion/extension of the elbow. It also has 6 passive joints to resolve the alignment problem. Both Ebrahimi's and Schiele's models have measurable joint positions required to obtain the Jacobian. Thus, GAEC can be applied to both models. However, simulation in this paper was carried out using Ebrahimi's model.

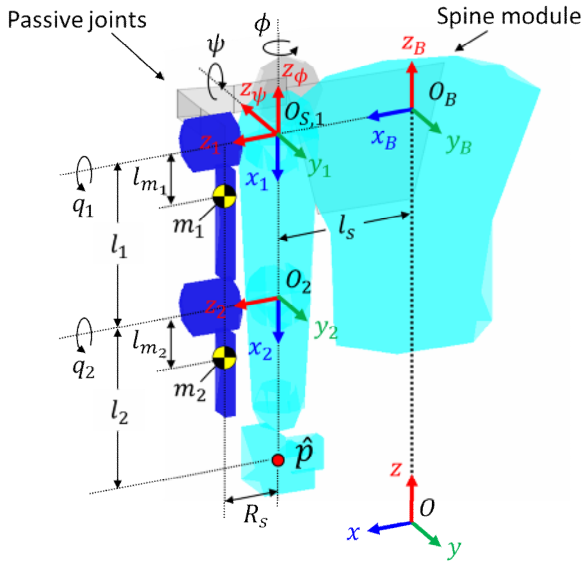


Fig. 4. Simulation model.

To simplify the problem, we made a few modifications and assumptions on the model of the robot and the user. First, the robot's active joints are sufficient to manage all the force in the work space. However, in order to show that the number of the active DOFs does not affect applicability of GAEC, the shoulder and elbow flexion/extension were assumed to be the only active DOFs. The orientation of the end-effector was assumed to be still measurable. Secondly, the shoulder was assumed as a ball joint with a fixed center of rotation. Finally, point $p$ was set to coincide with $\hat{p}$, and properties of the user arm (mass, length, etc.) were assumed to be known.

Fig. 4 shows the robot model. As shown, only the right arm was considered in the simulation. The user's body is also depicted to help the reader understand the model. In the figure, the base coordinate of the robot is $O_B$, and the coordinates of the active joints are $O_1$ and $O_2$. The coordinates of the passive joints are not included, because these DOFs depend completely on the user.

### *4.2 Controller implementation*

The robot torque $\tau_r$ in Eq. (1) for the simulation is obtained by Eq. (16) and dynamics of the actuator force control. It was assumed in the simulation that the actuator controller performs effectively, so that $\tau_r \approx \tau_d$.

Terminal sliding mode controller was selected as the position controller. It is known to be robust to parameter uncertainty and insensitive to disturbance, and also guarantee finite time convergence [38-42]. The terminal sliding surface was defined as

$$S = \dot{e} + Ce^{p_1/p_2} \tag{22}$$

where $e = q - q_0$, $C$ is a diagonal matrix composed of positive

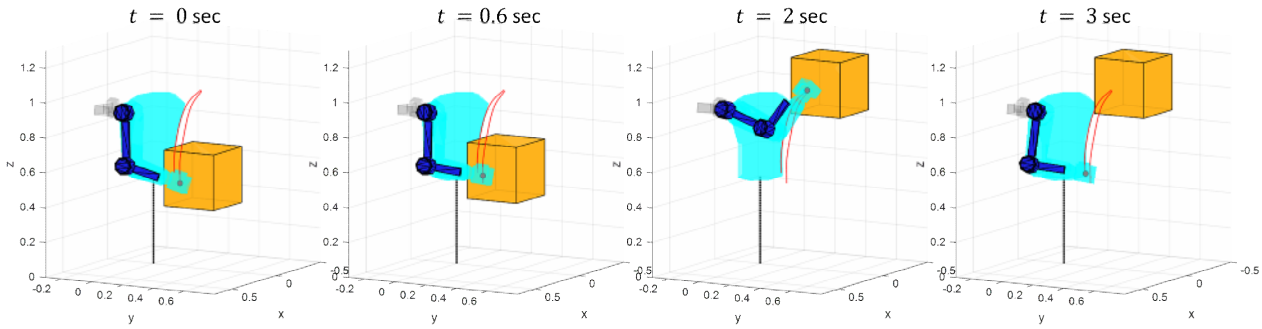


Fig. 5. Simulation scenario 1: Lifting and moving an object.

constants $c_1$ and $c_2$. And $p_1$ and $p_2$ are odd integers with $0 < p_1/p_2 < 1$ [37, 38]. The values of $p_1$ and $p_2$ were chosen as 3 and 5, respectively. The terminal sliding mode controller consists of equivalent control and discontinuous control [39]. The equivalent control was defined as

$$u_{eq} = D_0(q)\left(\ddot{q}_d - \tfrac{p_1}{p_2} C e^{p_1/p_2 - 1}\right) + C_0(q,\dot{q}) + g_0(q) \tag{23}$$

where $D_0 = D_r + D_h$, $C_0 = C_r + C_h$ and $g_0 = g_r + g_h$. For a positive constant $\psi$, the discontinuous control was defined as

$$\Delta u = \begin{cases} -\frac{S}{\delta}\omega & \text{if } \|S\| < \psi \\ -\frac{S}{\|S\|}\omega & \text{if } \|S\| \geq \psi \end{cases} \tag{24}$$

where $\omega$ is

$$\omega = \|S\| \left\|D_0^{-1}\right\| \left(b_0 + b_1\|q\| + \|\dot{q}\|^2\right). \tag{25}$$

and $b_0$, $b_1$ and $b_2$ are positive constants. In addition, a dissipation term was added to guarantee convergence of the external force estimator. The total terminal sliding controller is

$$u = u_{eq} + \Delta u - K\dot{e}\,. \tag{26}$$

The values of the shifting law parameters $\delta_1$, $t_1$, $\delta_2$, $\eta_m$, $\eta_d$ and $t_3$ were chosen by trial and error, which resulted in $\delta_1 = \delta_2 = 0.4$, $t_1 = 0.06$, $t_3 = 0.01$, $\eta_m = 0.1$ and $\eta_d = 0.01$. According to the value of $t_1$, the robot cannot be moved for at least 0.06 s between motions.

### *4.3 Scenario 1*

Scenario 1 involves lifting and moving a 5 kg object. The object is lifted and held for a little while, and then moved to a higher location, as shown in Fig. 5, where the red line represents the trajectory of $\hat{p}$. This scenario is designed for simulating weight handling activities, such as manipulating a heavy tool. Simulation of this scenario shows how GAEC works for such activities.

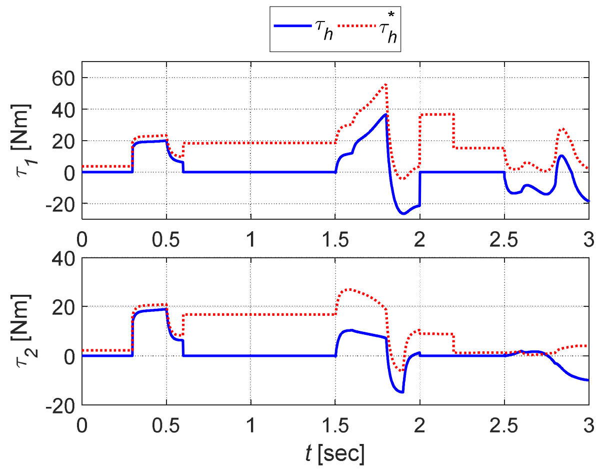


Fig. 6. The user's torque for scenario 1. $\tau_1$ and $\tau_2$ denote flexion/extension torque on the shoulder and elbow, respectively.

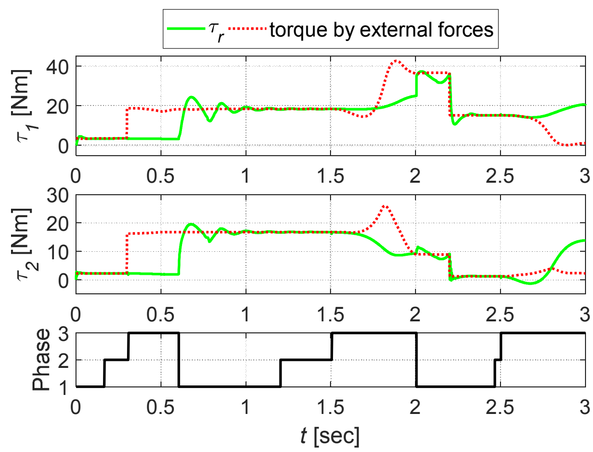


Fig. 7. The robot's torque for scenario 1. $\tau_1$ and $\tau_2$ denote the flexion/extension torque on the shoulder and elbow, respectively. In the phase plot, 1, 2 and 3 refer to phases I, II and III, respectively.

Fig. 6 shows $\tau_h$ and $\tau_h^*$ for the scenario. Fig. 7 shows the robot torque $\tau_r$ and the torque by the external forces, and the cycle of phase for the same work. Note that the torque by the external forces is shown in the opposite sign, because it is the target of $\tau_r$. Initially, the weights of the human arm and the

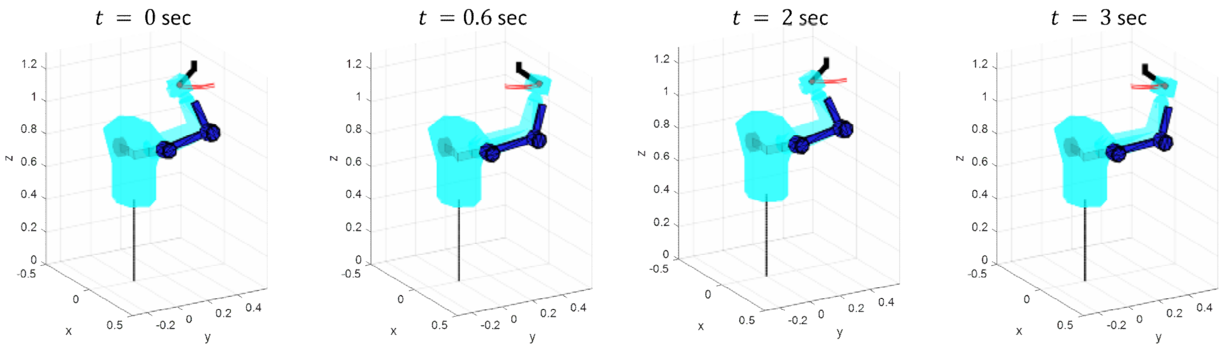


Fig. 8. Simulation scenario 2: Tightening a bolt.

robot itself were compensated. The object is lifted from 0.3 to 0.6 s, for which the weight of the object is not on the robot because it is supported by the user only.

The object is held from 0.6 to 1.5 s. At 0.6 s, the user's torque is relieved and the robot starts to neutralize the weight of the object. Because the weight of the object is compensated for by the robot, the object can be held without the user's effort for the period.

The object is moved to a higher target location from 1.5 to 2 s, for which less torque is required for the user. It is noted that magnitude of $\tau_h$ is larger than that of $\tau_h^*$ from about 1.8 to 2 s. This is because force in the same direction as the external force (weight of the object) is required for the period. As the weight of the object is compensated for by the robot, the user has to apply force against the compensation force.

The moving motion ends at 2 s and the object is put down at 2.2 s. The external force neutralization process is repeated in case of a situation change. The user returns to the initial posture from 2.5 s to 3 s. The magnitude of $\tau_h$ is larger than that of $\tau_h^*$ for this period because the robot's compensatory force, which is the weight of the user and robot combined, remains same as that at 2.5 s.

Additional inertia by the object causes fluctuation of $\tau_r$ to start at 0.6 s in phase I. The problem is undesirable because it may delay completion of phase I and make the user unmovable during phase I. By improving robustness of the position controller, it is possible to prevent delay of completion of phase I.

### 4.4 Scenario 2

Scenario 2 involves fastening a bolt with a wrench, as shown in Fig. 8, where the red line represents the trajectory of $\hat{p}$. This scenario was inspired by the overhead work required in car assembly lines. In this scenario, a 50 N force is applied to the wrench handle and then the wrench is pushed to fasten the bolt. Then, the force is released, and the wrench is returned to its initial position. It is possible to apply force by pushing with the user's body weight while posture of the arm is fixed. This scenario corresponds to general pushing/pulling activities. Various activities can be done in a similar fashion, for example, grinding, drilling, and punching with power tools in the manufacturing field.

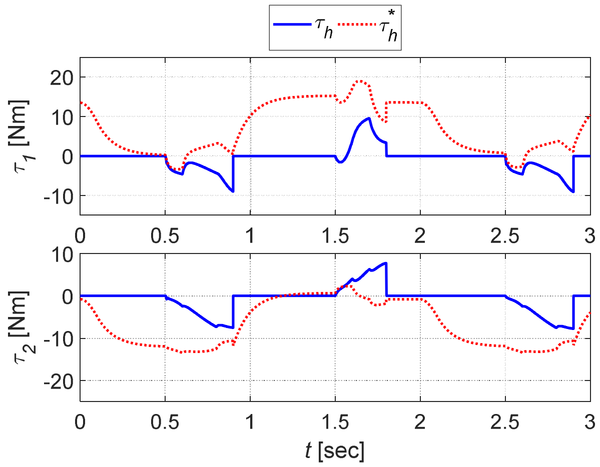


Fig. 9. The user's torque for scenario 2. $\tau_1$ and $\tau_2$ denote the flexion/extension torque on the shoulder and elbow, respectively.

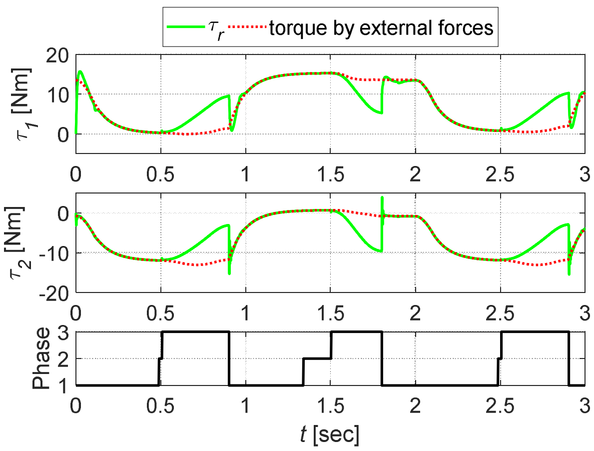


Fig. 10. The robot's for scenario 2. $\tau_1$ and $\tau_2$ denote the flexion/extension torque on the shoulder and elbow, respectively. In the phase plot, 1, 2 and 3 refer to phases I, II and III, respectively.

Fig. 9 shows the user's torque $\tau_h$ and $\tau_h^*$. Fig. 10 shows $\tau_r$, torque by the external forces, and cycle of the phases for scenario 2. For 0 – 0.5 s, the user applies a 50 N force gradually to the wrench handle along the +y-direction. The force is applied by the body weight with the arm posture fixed. As the robot generates torque to maintain the arm posture in that process, the user's effort is not needed. For 0.5 – 0.9 s, the wrench is turned by approximately 60° around the +z-axis. The only torque required for the user is the inertia and residual force, since the torque necessary to apply 50 N on the arm is maintained by the robot.

The 50 N force is released at 0.9 s and the neutralization process is repeated. It can be observed that the torque on the user's shoulder required by the overhead posture is compensated by the robot. From 1.5 s to 1.8 s, the user's initial posture is recovered. Here in scenario 2 again, the user needs to overcome only the inertia and residual force. The wrench-turning process is restarted at 2 s.

## 5. Conclusion

In order to overcome limitations of existing exoskeleton robots in terms of independence from robot platforms and capability for general purposes, a control scheme named GAEC was designed for upper limb exoskeleton robots. GAEC can assist the human worker's common activities working in the two modes by neutralizing a step-like external force and complying the user's own force. Performance of GAEC was validated by computer simulation of two scenarios featuring two of the most common working activities. On condition that the user understands the working process of GAEC and the robot's joint position information is available, GAEC can be used for general purposes without dependence on the type of robot platform.

One of the main advantages of GAEC is that it does not require a sensor system to estimate the user's motion intention. As it requires the joint position information only, the exoskeleton platform can include more active DOFs at a lower price without concerns on sensor location. In addition, the capability for general purposes of GAEC is expected to promote development of exoskeleton platforms that can be used in various fields and also specialized for a specific field by an add-on application.

Some practical issues with GAEC may be discussed. For robots with a complex joint mechanism or several joints, it may be difficult or expensive to measure all the joint positions. In this case, GAEC can be complemented by employing an acceleration measurement device, such as an inertia measurement unit (IMU). Another issue is that the phase shifting law may be affected by measurement noise of the position. In order to avoid the problem, noise filtering can be as important as determining the shifting law constants.

## Acknowledgments

This research was supported by Basic Science Research Program through the National Research Foundation of Korea (NRF) funded by the Ministry of Education (2018R1D1 A1B07047744).

## References


[1] K. Kiguchi and Q. Quan, Muscle-model-oriented EMG-based control of an upper-limb power-assist exoskeleton with a neuro-fuzzy modifier, *IEEE International Conference on Fuzzy Systems* (2008) 1179-1184.

[2] T. Koyama, T. Tanaka, S. Kaneko, S. Moromugi and M. Q. Feng, Integral ultrasonic muscle activity sensor for detecting human motion, *IEEE International Conference on Systems, Man and Cybernetics* (2005) 1669-1674.

[3] Z. Li, Z. Huang, W. He and C. Y. Su, Adaptive impedance control for an upper limb robotic exoskeleton using biological signals, *IEEE Transactions on Industrial Electronics,* 64 (2) (2017) 1664-1674.

[4] H. Choi and S. Lee, Classification of hand postures using forearm perimeter sensor and compensation of residual muscle volume change with sEMG, *International Journal of Mechatronics and Automation*, 4 (4) (2017) 213-221.

[5] L. Peternel, T. Noda, T. Petrič, A. Ude, J. Morimoto and J. Babič, Adaptive control of exoskeleton robots for periodic assistive behaviours based on EMG feedback minimisation, *PloS One,* 11 (2) (2016).

[6] B. Brahim, S. Maarouf, C. O. Luna, B. Abdelkrim and M. H. Rahman, Adaptive iterative observer based on integral backstepping control for upper extremity exoskelton robot, *8th International Conference on Modelling, Identification and Control* (2016) 886-891.

[7] A. Ebrahimi, Stuttgart exo-jacket: An exoskeleton for industrial upper body applications, *10th International Conference on Human System Interactions* (2017) 258-263.

[8] A. Ebrahimi, D. Gröninger, R. Singer and U. Schneider, Control parameter optimization of the actively powered upper body exoskeleton using subjective feedbacks, *3rd International Conference on Control, Automation and Robotics* (2017) 432-437.

[9] J. Garrido, W. Yu and X. Li, Modular design and control of an upper limb exoskeleton, *Journal of Mechanical Science and Technology,* 30 (5) (2016) 2265-2271.

[10] J. Huang, W. Huo, W. Xu, S. Mohammed and Y. Amirat, Control of upper-limb power-assist exoskeleton using a human-robot interface based on motion intention recognition, *IEEE Transactions on Automation Science and Engineering,* 12 (4) (2015) 1257-1270.

[11] H. D. Lee, B. K. Lee, W. S. Kim, J. S. Han, K. S. Shin and C. S. Han, Human–robot cooperation control based on a dynamic model of an upper limb exoskeleton for human power amplification, *Mechatronics,* 24 (2) (2014) 168-176.

[12] T. Madani, B. Daachi and K. Djouani, Modular-controller-design-based fast terminal sliding mode for articulated exoskeleton systems, *IEEE Transactions on Control Systems Technology,* 25 (3) (2017) 1133-1140.

[13] S. Oh, K. Kong and Y. Hori, Design and analysis of force-

sensor-less power-assist control, *IEEE Transactions on Industrial Electronics,* 61 (2) (2014) 985-993.

[14] T. Rogge, U. Daub and A. Ebrahimi, Status demonstration of the interdisciplinary development regarding the upper limb exoskeleton. Stuttgart exo-jacket, *Internationales Stuttgarter Symposium* (2017) 1317-1329.

[15] R. Steger, S. H. Kim and H. Kazerooni, Control scheme and networked control architecture for the Berkeley lower extremity exoskeleton (BLEEX), *IEEE International Conference on Robotics and Automation* (2006) 3469-3476.

[16] A. B. Zoss, H. Kazerooni and A. Chu, Biomechanical design of the Berkeley lower extremity exoskeleton (BLEEX), *IEEE/ASME Transactions on Mechatronics,* 11 (2) (2006) 128-138.

[17] J. B. Huang, K. Y. Young and C. H. Ko, Effective control for an upper-body exoskeleton robot using ANFIS, *International Conference on System Science and Engineering* (2016) 1-4.

[18] K. Kim, K. J. Hong, N. G. Kim and T. K. Kwon, Assistance of the elbow flexion motion on the active elbow orthosis using muscular stiffness force feedback, *Journal of Mechanical Science and Technology,* 25 (12) (2011) 3195-3203.

[19] T. Noda, T. Teramae, B. Ugurlu and J. Morimoto, Development of an upper limb exoskeleton powered via pneumatic electric hybrid actuators with bowden cable, *2014 IEEE/RSJ International Conference on Intelligent Robots and Systems* (2014) 3573-3578.

[20] J. C. Perry, J. Rosen and S. Burns, Upper-limb powered exoskeleton design, *IEEE/ASME Transactions on Mechatronics,* 12 (4) (2007) 408-417.

[21] A. Riani, T. Madani, A. El Hadri and A. Benallegue, Adaptive integral terminal sliding mode control of an upper limb exoskeleton, *18th International Conference on Advanced Robotics* (2017) 131-136.

[22] H. Seo and S. Lee, Design and experiments of an upper-limb exoskeleton robot, *International Conference on Ubiquitous Robots and Ambient Intelligence* (2017) 807-808.

[23] F. Xiao, Y. Gao, Y. Wang, Y. Zhu and J. Zhao, Design and evaluation of a 7-DOF cable-driven upper limb exoskeleton, *Journal of Mechanical Science and Technology,* 32 (2) (2018) 855-864.

[24] A. Schiele, *Fundamentals of Ergonomic Exoskeleton Robots*, Ph.D. Thesis, Delft University of Technology, Delft, The Netherlands (2008).

[25] R. A. R. C. Gopura, D. S. V. Bandara, K. Kiguchi and G. K. I. Mann, Developments in hardware systems of active upper-limb exoskeleton robots: A review, *Robotics and Autonomous Systems,* 75 (2016) 203-220.

[26] R. A. R. C. Gopura, D. S. V. Bandara, J. M. P. Gunasekara and T. S. S. Jayawardane, Recent trends in EMG-Based control methods for assistive robots, *Electrodiagnosis in New frontiers of Clinical Research*, InTech (2013) 237-268.

[27] A. Concha, F. E. G. Sánchez, E. R. Velasco, M. Sánchez and S. K. Gadi, Comparison of control algorithms using a generalized model for a human with an exoskeleton, *Journal of Applied Science & Process Engineering,* 5 (1) (2018) 249-255.

[28] C. Dahmen, C. Hölzel, F. Wöllecke and C. Constantinescu, Approach of optimized planning process for exoskeleton centered workplace design, *Procedia CIRP,* 72 (2018) 1277-1282.

[29] K. S. Stadler and D. Scherly, Exoskeletons in industry: Designs and their potential, *8th International Symposium on Automatic Control*, Wismar, Germany (2017).

[30] J. Ortiz, E. Rocon, V. Power, A. de Eyto, L. O'Sullivan, M. Wirz, C Bauer, S. Schülein, K. S. Stadler, B. Mazzolai, W. B. Teeuw, C. Baten, C. Nikamp, J Buurke, F. Thorsteinsson and J. Müller, XoSoft - A vision for a soft modular lower limb exoskeleton, *Wearable Robotics: Challenges and Trends*, 16 (2017).

[31] R. F. Natividad and C. H. Yeow, Development of a soft robotic shoulder assitive device for shoulder abduction, *IEEE International Conference on Biomedical Robotics and Biomechatronics* (2016) 989-993.

[32] J. Ortiz, T. Poliero, G. Cairoli, E. Graf and D. G. Caldwell, Energy efficiency analysis and design optimization of an actuation system in a soft modular lower limb exoskeleton, *IEEE Robotics and Automation Letters*, 3 (1) (2018) 484-491.

[33] M. Wehner, B. Quinlivan, P. M Aubin, E. Martinez-Villalpando, M. Baumann, L. Stirling, K. Holt, R. Wood and C. Walsh, A lightweight soft exosuit for gait assistance, *IEEE International Conference on Robotics and Automation* (2013).

[34] J. Li, Y. Lu, Y. Nan, L. He, X. Wang and D. Niu, A study on posture analysis of assembly line workers in a manufacturing industry, *Proceedings of the 20th Congress of the International Ergonomics Association* (2018).

[35] S. R. Kamat, N. E. N. Md Zula, N. S. Rayme, S. Shamsuddin and K. Husain, The ergonomics body posture on repetitive and heavy lifting activities of workers in aerospace manufacturing warehouse, *IOP Conference Series: Materials Science and Engineering*, 210 (1) (2017).

[36] N. Sylla, V. Bonnet, F. Colledani and P. Fraisse, Ergonomic contribution of ABLE exoskeleton in automotive industry, *International Journal of Industrial Ergonomics*, 44 (4) (2014), 475-481.

[37] A. Schiele and Gerd Hirzinger, A new generation of ergonomic exoskeletons – The high-performance X-arm-2 for space robotics telepresence, *IEEE/RSJ International Conference on Intelligent Robots and Systems* (2011) 2158-2165.

[38] Y. Feng, X. Yu and Z. Man, Non-singular terminal sliding mode control of rigid manipulators, *Automatica,* 38 (12) (2002) 2159-2167.

[39] S. Venkataraman and S. Gulati, Control of nonlinear systems using terminal sliding modes, *Journal of Dynamic Systems, Measurement and Control,* 115 (3) (1993) 554-560.

[40] M. Zhihong, A. P. Paplinski and H. R. Wu, A robust MIMO terminal sliding mode control scheme for rigid robotic manipulators, *IEEE Transactions on Automatic Con-*

*trol,* 39 (12) (1994) 2464-2469.
[41] K. B. Park and J. J. Lee, A robust MIMO terminal sliding mode control scheme for rigid robotic manipulators-Comments, *IEEE Transactions on Automatic Control,* 41 (5) (1996) 761-762.
[42] M. B. R. Neila and D. Tarak, Adaptive terminal sliding mode control for rigid robotic manipulators, *International Journal of Automation and Computing,* 8 (2) (2011) 215-220.
[43] J. J. E. Slotine and W. Li, *Applied Nonlinear Control*, Prentice hall Englewood Cliffs (1991).
[44] M. W. Spong, S. Hutchinson and M. Vidyasagar, *Robot Modeling and Control*, Wiley, New York, USA (2006).

**Hwiwon Seo** received the B.S. degree in mechanical engineering at Konkuk University, Seoul, South Korea in 2017. He is currently pursuing his M.S. degree in mechanical design and production engineering at Konkuk University. His research interests include robotics, control and exoskeleton robots.

**Sangyoon Lee** received the Ph.D. degree in mechanical engineering at Johns Hopkins University in 2003. Since then, he has been a Professor at Konkuk University. He is serving as a Director for Korean Society of Mechanical Engineers and Korea Robotics Society. His research interests include robotics, control, and printed electronics.